Avrupa Bilim ve Teknoloji Dergisi
Özel Sayı 24, S. 474-478, Nisan 2021

Araştırma Makalesi

www.ejosat.com ISSN:2148-2683

European Journal of Science and Technology
Special Issue 24, pp. 474-478, April 2021

Research Article

Near-Zero-Index Split Ring Resonator: A Lens Antenna

İsmail Yıldız[1], Turgut İkiz[2], Şule Çolak[3], Faruk Karadağ[4], Muharrem Karaaslan[5], Duygu Nazan Gençoğlan*[6]

[1] Çukurova University, Dept. of Electrical and Electronics Engineering, Adana, Turkey,0000-0000-0000-0000, ismailyildiz82@gmail.com
[2] Çukurova University, Dept. of Electrical and Electronics Engineering, Adana, Turkey, 0000-0002-0197-5761, tikiz@cu.edu.tr
[3] Adana Alparslan Turkes Science and Technology University, Dept. of Electrical and Electronics Engineering, Adana, Turkey, 0000-0002-9529-4544, scolak@atu.edu.tr
[4] Çukurova University, Dept. of Physics, Adana, Turkey, 0000-0001-7862-9085, fkaradag@cu.edu.tr
[5] İskenderun Technical University, Dept. of Electrical and Electronics Engineering, Hatay, Turkey, 0000-0003-0923-1959, muharrem.karaaslan@iste.edu.tr
[6*] Adana Alparslan Turkes Science and Technology University, Dept. of Electrical and Electronics Engineering, Adana, Turkey, 0000-0001-5014-9514, dngencoglan@atu.edu.tr

(2nd International Conference on Access to Recent Advances in Engineering and Digitalization (ARACONF)-10–12 March 2021)

(**DOI:** 10.31590/ejosat.903929)

ATIF/REFERENCE: Yıldız, İ, İkiz, T., Çolak, Ş., Karadağ, F., Karaaslan, M. & Gençoğlan, D.N. (2021). Near-Zero-Index Split Ring Resonator: A Lens Antenna. *European Journal of Science and Technology*, (24), 474-478.

Abstract

In this study, a matematerial structure, which consists of rectangular split ring resonator arrays, is investigated numerically and experimentally in the frequency range from 1 GHz to 5GHz. FR-4 material is used as the substrate material due to its low cost. During the numerical analysis (simulation analysis), a parametric study is performed to determine the optimal dimension of the unit cell structure. S_{11} (reflection coefficient), S_{21} (transmission coefficient), and n (refractive index) are examined in the frequency range of interest. As a result of the parametric study, the value of n is obtained as approximately zero. By increasing the split ring width, near-zero index is observed at higher frequencies. Hence, it is also deduced that the metamaterial structure behaves as a super lens antenna at the related frequency. Numerical analysis is performed via CST Microwave Studio (MWS). The simulation results are confirmed with experimental results obtained by network analyzer.

Keywords: Split Ring Resonator, Super Lens Antennas, Metamaterials, MEMS

Sıfıra Yakın İndeksli Ayrık Halka Resonatörü: Lens Anten

Öz

Bu çalışmada dikdörtgen bölünmüş halkalı rezonatör dizilerinden oluşan bir malzeme yapısı 1 GHz ile 5 GHz frekans aralığında sayısal ve deneysel olarak incelenmiştir. Düşük maliyeti nedeniyle FR-4 malzemesi alt tabaka malzemesi olarak kullanılmıştır. Sayısal analiz (simülasyon analizi) sırasında, tek hücre yapısının optimal boyutunu belirlemek için parametrik çalışma yapılmıştır. İlgili frekans aralığında S_{11} (yansıma katsayısı), S_{21} (iletim katsayısı) ve n (kırılma indisi) incelenmiştir. Parametrik çalışma sonucunda, *n* değeri yaklaşık sıfır olarak elde edilmiştir. Bölünmüş halka genişliği artırılarak, daha yüksek frekanslarda sıfıra yakın indeks gözlemlenmiştir. Dolayısıyla, metamalzeme yapısının ilgili frekansta bir süper lens (mercek) anten gibi davrandığı da saptanmıştır. Sayısal analiz CST Microwave Studio (MWS) aracılığıyla gerçekleştirilmiştir. Simülasyon sonuçları, ağ analizörü ile elde edilen deneysel sonuçlarla doğrulanmıştır.

Anahtar Kelimeler: Ayrık Halka Rezonatörü, Süper Lens(Mercek) Anten, Metamalzemeler, MEMS

1. Introduction

In recent years, metamaterials, artificial materials not found in nature, have been the subject of attention for most researchers. The idea of negative values of permittivity ε, permeability μ and refractive index n put forward by Veselago (Veselago, 1968) was first theoretically proved by Pendry (Pendry et al., 1999). Smith et al. (Smith and Croll, 2000; Smith et al., 2004) first produced the materials which could be designed with the desired electromagnetic properties. These structures are used in many application areas such as cloaking (Cai et al., 2007; Schuring, 2006), sensing (Altıntaş et al., 2019; Abdulkarim, 2019; Bakır et al., 2019; Talai et al., 2017), antennas (Abdalla, 2017; Hamad, 2019; Kawdungta, 2017; Fu et al., 2016; Salamin et al., 2020; Mark, et al., 2020; Mishra et al., 2019), energy harvesting (Zeng et al., 2019; Wang et al., 2015; Bağmancı et al., 2019; Bağmancı et al., 2019; Haque et al., 2015), and super lens (Khoomwong and Phongcharoenpanich, 2017; Li et al., 2016; Orazbayev et al., 2015; Pen et al., 2019). Several studies concerning metamaterials have been performed in microwave frequencies, THz frequencies (Abbas et al., 2020), infrared and optical ranges. Metamaterials are widely manufactured by periodically placing metal elements on a substrate. The metal elements on the substrate can have many different geometries or forms. The split ring resonators (SRR) (Sabah and Roskos, 2012) are the most commonly used structures in the production of metamaterials. The split ring resonators consist of two intertwined metal strips and splits on the metal strips. The split ring resonator unit is an artificial magnetic resonator which resonates at a frequency with a wavelength λ_0 that is much larger than the split ring resonator length. The split ring resonators shows inductive effect due to metallic parts and capacitive effect due to split and cavity parts. Therefore, the split ring resonators can be modeled as LC circuits. The metamaterial sensor applications created by using the split ring resonator are mainly based on sensing the variations in the parameters by observing changes in the resonance frequency of the metamaterial sensor. The remarkable variation in resonant frequency of a resonator depends on the values of the capacitance and the inductance of the resonator. The split ring resonator-based metamaterials are produced by placing metal resonators in different shapes by using printed circuit technique on the substrate. The split ring resonator can be of different types according to its geometry, depending on the state of the metal parts and cavities, for example complementary split ring resonator (Reddy and Raghavan, 2013; Karimzadeh et al., 2007).

Inasmuch as its wide operating band, high directivity, low production cost, and simple processing etc., the lens antenna has got considerably attention in communication systems, radar applications and space technology (Boybay and Ramahi, 2012). The conventional array antennas possess complicated feed network, the reflector antenna is not compact and difficult to integrate into any surfaces. The lens antenna tackles the deficiencies of the above two types of antennas as well as having high directivity. However, the specific form of the classic lens will increase the complexity of the machining process, and is not easy to install. With the rapid improvement on the millimeter and sub-millimeter wave circuit technology in recent years, there has been a renovated attention on lens antennas (Fernandes et at., 2016), which exhibit a more reasonable dimension at these frequencies. Lenses can be used to make a change in the phase and/or the amplitude of the main feed radiation pattern for the purpose of exchanging a certain output radiation pattern.

A Microelectromechanical system (MEMS) is the technology of tiny size mechanical devices with leastways a few of their dimensions in the micrometer range are tilled by electricity. Generally, a central unit arises that processes the data, the microprocessor, and many components that interact with the outside (Sauleau et al., 2005). MEMS provide a very good facility for applications in the dispatch or control of industrial systems and processes. Their advantages of small size, low cost, high sensitivity, and small power consumption make them excellent renewals of preceding macro size components. Furthermore, several applications are just feasible in the case at the micrometer scale (Mamilla and Chakradhar, 2014). The split width, correspondingly the frequency range where refractive index n goes to zero can be controlled by using the MEMS.

In this study, for the rectangular split ring resonators, the variations of the reflection coefficient S_{11}, the transmission coefficient S_{21} and the refractive index n according to the width of the split of the resonator are examined numerically and experimentally. In numerical analysis, the proposed structure is simulated at 1-5 GHz frequency range by using CST Microwave Studio Program. Specifically, the variation of refractive index of the proposed structure due to variation of the splits has been investigated. The graphs of the reflection coefficient, the transmission coefficient and the refractive index are obtained clearly. The reflection coefficient and the transmission coefficient of the proposed structure is fabricated and then measured by using the vector network analyzer. The results obtained both numerically and experimentally are compared with each other.

2. Design and Simulation

The proposed structure is shown in Fig.1 with its front and back views. It consists of a rectangular split ring resonator with splits in opposite directions, and a strip is placed behind the FR-4 substrate being perpendicular to the splits of the resonator. The dimension of the used FR-4 based metamaterial structure is 10 mm x10 mm x1.6 mm. The metallic parts of the resonator and strip behind the substrate are made up of copper material with thickness of 0.035 mm. The strips of the resonator and the strip behind the substrate have a width of 0.7 mm and the distance between the strips of the resonator is 0.8 mm. The longest side of the outer strip of the resonator is 9 mm and the inner strip has longest size of 6 mm. The splits of the resonator are identical and dimensions of splits are swept from 0.5 mm to 2 mm with steps of 0.5 mm. The strip perpendicular to the splits has a length of 9.8 mm.

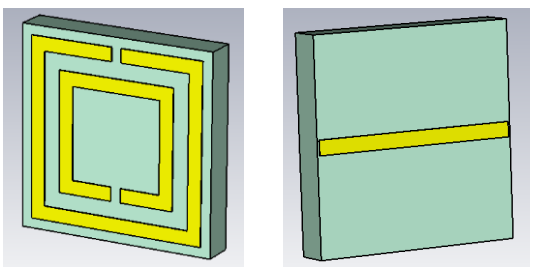

Figure 1: Front and back view of the structure

The proposed structure is simulated by using CST MWS simulation program in the frequency range of 1-5 GHz. In simulation, the resonator width of splits is varied from 0.5 mm to 2 mm. Then, s-parameters and refractive index n are observed and investigated for each case.

The graph of the reflection coefficient S_{11} is shown in Fig.2. It is clear that the resonance frequency of the resonator increases while the width of the splits increases. The reflection coefficient goes to zero rapidly at 2.15 GHz when the split width is 0.5 mm. The resonance frequency increases to 2.22, 2.28 and 2.33 GHz while the width is 1, 1.5, and 2 mm respectively.

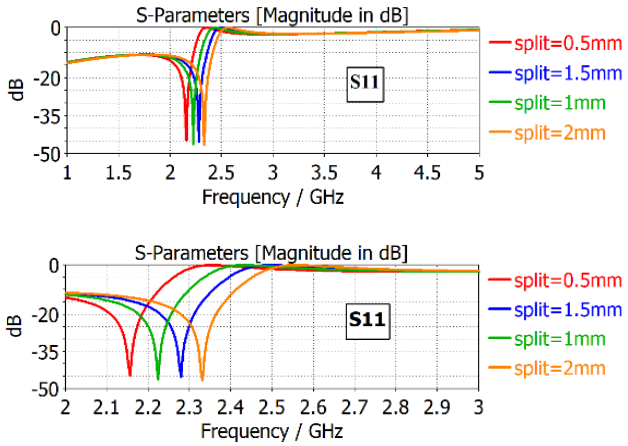

Figure 2: Graph of variation of S_{11} parameter with different split widths in the simulation

The transmission coefficient S_{21} for different split widths can be seen in Fig.3. It is also clear from Figure 3 that he transmission coefficient S_{21} is compatible with the result of S_{11} graph. That is, the resonance frequency of the resonator increases while the width of the split increases. The transmission coefficient goes to zero rapidly at 2.35 GHz when the split width is 0.5 mm. The frequency increases to 2.43, 2.49 and 2.56 GHz while the width is 1, 1.5, and 2 mm respectively.

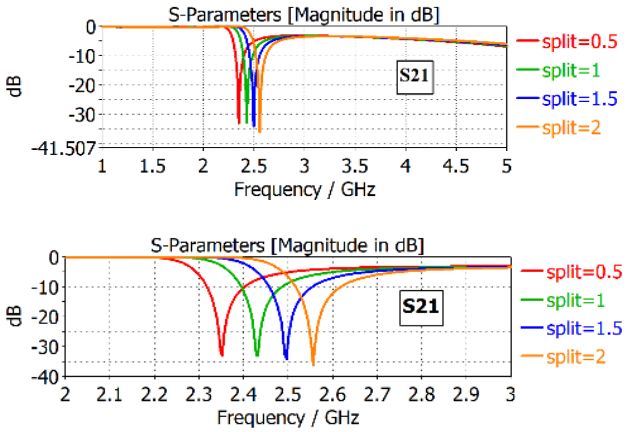

Figure 3: Graph of variation of S_{21} parameter with different split widths in the simulation

The graph of the refractive index *n* is shown in Fig.4. As it can be seen from below graph, *n* is very close to zero in a certain frequency range and this range shifts to higher frequencies when the width increases. When the width of the split is 0.5, the refractive index *n* very closed to zero in the frequency range 2.35-2.65 GHz in 300 MHz frequency band. When the width is 1, 1.5 and 2 mm, the frequency range is 2.45-2.75 GHz, 2.52-2.82 GHz and 2.6-2.9 GHz respectively.

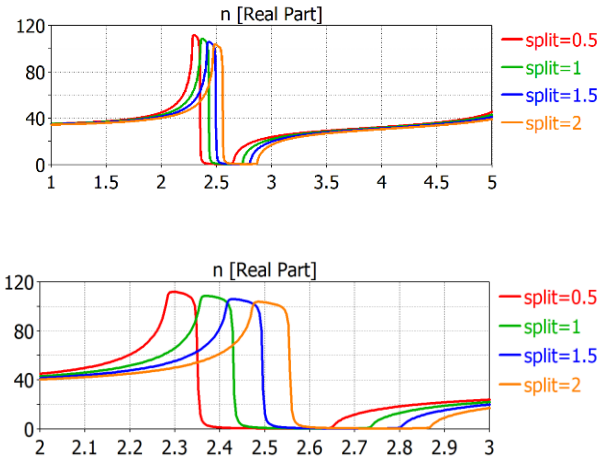

Figure 4: Graph of variation of *n* parameter with different split widths in the simulation

In this part, it is outlined that the value of *n* is obtained as approximately zero. In other words, it is deduced that the proposed structure behaves as a super-lens antenna in the frequency range from 2.35 GHz to 2.65 GHz. While the width of the splits increases, the near zero index shifts towards higher frequencies. By using the MEMS, the width of the split can be arranged for desired width, so the proposed structure can work as a lens antenna in the desired frequency range.

3. Fabrication and Measurement

In order to verify the simulation results, the proposed structure is fabricated by using LPKF Proto-Mat E33 and a common printed circuit board method. The unit cell of the structure has the dimension of 10x10 mm^2. The fabricated structure is composed of 18x18 unit cells. This is because the largest dimension of the horn is 16 cm and the structure must be bigger than the largest dimension of the horn. The fabricated structure is shown in Fig. 5.

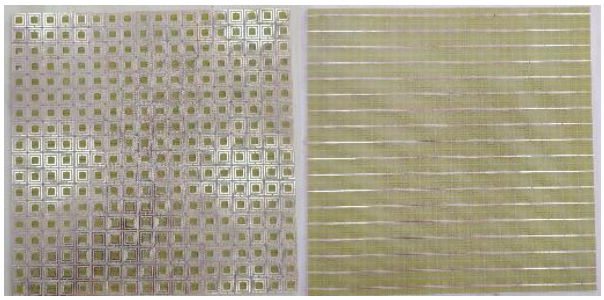

Figure 5: Front and back view of the structure produced with 18x18 unit cells

Agilent PNA-L series vector network analyzer (VNA) and a linearly polarized standard gain horn antenna which works at the 2-4.8 GHz frequency range with the aperture dimensions of 13-16 cm are used to measure the reflection coefficient S_{11} and the transmission coefficient S_{21}. Fig. 6 shows the experimental setup.

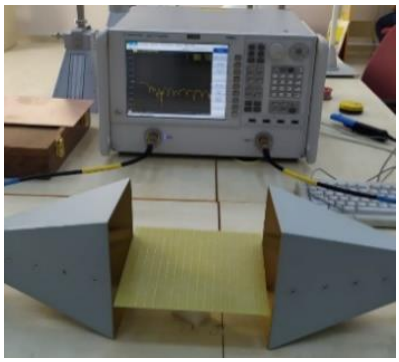

Figure 6: Experimental Setup

The experimental data is transferred to computer, and the graphs of S_{11} and S_{21} are obtained by using MATLAB program in order to compare with numerical results. Both simulation and experiment graphs of the reflection coefficient S_{11} and the transmission coefficient S_{21} are obtained and sketched simultaneously as shown in Fig. 7.

4. Results and Discussion

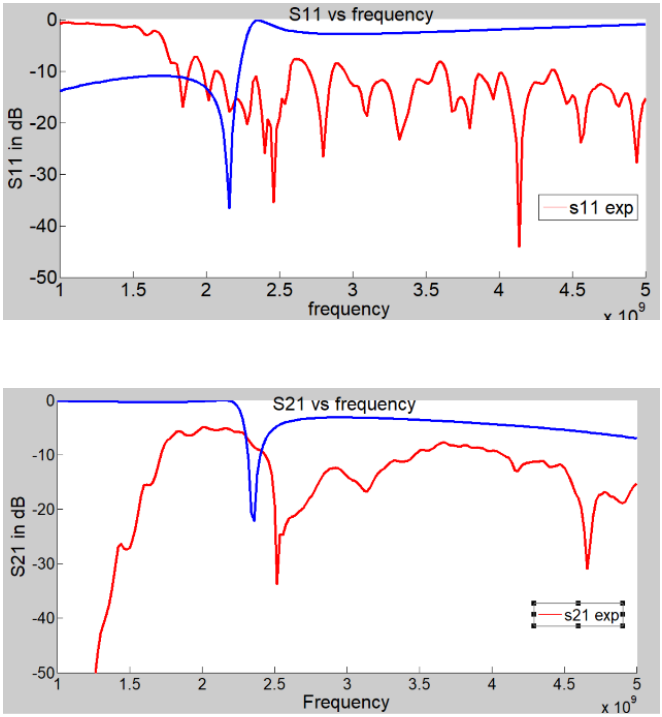

Figure 7: Simulation and experiment results of S_{11} and S_{21}

As can be seen clearly from Fig. 7, the graphs of S_{11} and S_{21} obtained by simulation and experimental analysis are in good agreement. Based on these results, it can be said that the simulation is confirmed experimentally. Numerical and experimental results are not compatible below 2 GHz and above 4.5 GHz. Because the antennas used in the experiment operate in the frequency range of 2-4.8 GHz.

5. Conclusion and Recommendations

In this work, a matematerial structure consisting of rectangular split ring resonators is investigated numerically and experimentally according to the variation of the split of the resonator. The variations of the reflection coefficient S_{11}, the transmission coefficient S_{21} and the refractive index *n* are given graphically and interpreted clearly. The numerical results of s-parameters are confirmed experimentally.

As can be seen from the numerical and experimental results, *n*, refractive index parameter, is very close to zero within a certain frequency range. It means that the proposed structure is obtained as a super lens antenna in the frequency range of interest. The frequency ranges in which the *n* parameter decreases to zero with the change in the width of the splits shift in proportional to the split's variation. This result allows the structure to be used as a mechanically adjustable antenna. In other words, the proposed structure is controlled by MEMS (MEMS based metamaterial structure). By adjusting the width of the splits, the antenna structure radiates efficiently in the desired frequency range.

5. Acknowledge

This work was supported by the by the Scientific Research Projects Unit (BAP) In Çukurova University. Project No: 12479. Project Title: Design and Characterization of Split Ring Resonators for Antenna and Sensor Applications.

References

Abbas, A. A., El-Absi, M., Abuelhaija, A., Solbach, K., Kaiser, T. (2020). Wide-Angle RCS Enhanced Tag Based on Dielectric Resonator–Lens Combination. *Frequenz*, *74*(1-2), 1-8.

Abdalla, M. A., Ibrahim, A. A. (2017). Simple μ-negative half mode CRLH antenna configuration for MIMO applications. *Radioengineering*, *26*(1), 45-50.

Abdulkarim, Y. I., Deng, L., Altıntaş, O., Ünal, E., Karaaslan, M. (2019). Metamaterial absorber sensor design by incorporating swastika shaped resonator to determination of the liquid chemicals depending on electrical characteristics. *Physica E: Low-dimensional Systems and Nanostructures*, *114*, 113593.

Abdulkarim, Y. I., Deng, L., Karaaslan, M., Unal, E. (2019). Determination of the liquid chemicals depending on the electrical characteristics by using metamaterial absorber based sensor. *Chemical Physics Letters*, *732*, 136655.

Altintaş, O., Aksoy, M., Ünal, E., Karaaslan, M. (2019). Chemical liquid and transformer oil condition sensor based on metamaterial-inspired labyrinth resonator. *Journal of The Electrochemical Society*, *166*(6), B482.

Bağmancı, M., Akgöl, O., Özaktürk, M., Karaaslan, M., Ünal, E., Bakır, M. (2019). Polarization independent broadband metamaterial absorber for microwave applications. *International Journal of RF and Microwave Computer-Aided Engineering*, *29*(1), e21630.

Bağmancı, M., Karaaslan, M., Unal, E., Özaktürk, M., Akgol, O., Karadağ, F., Bakır, M. (2019). Wide band fractal-based perfect energy absorber and power harvester. *International Journal of RF and Microwave Computer-Aided Engineering*, *29*(7), e21597.

Bakır, M., Karaaslan, M., Karadag, F., Dalgac, S., Ünal, E., Akgöl, O. (2019). Metamaterial Sensor for Transformer Oil, and Microfluidics. *Applied Computational Electromagnetics Society Journal*, *34*(5).

Boybay, M. S., Ramahi, O. M. (2012). Material characterization using complementary split-ring resonators. *IEEE Transactions on instrumentation and Measurement*, *61*(11), 3039-3046.

Cai, W., Chettiar, U. K., Kildishev, A. V., Shalaev, V. M. (2007). Optical cloaking with metamaterials. *Nature photonics*, *1*(4), 224-227.

Fernandes, C. A., Lima, E. B., Costa, J. R. (2016). Dielectric lens antennas. *Handbook of antenna technologies*, 1001-1064.

Fu, Q., Fan, C. L., Li, S. J., Wang, G., Cao, X. Y. (2016). Ultra-broad band radar cross section reduction of waveguide slot antenna with metamaterials. *Radioengineering*, *25*(2), 241.

Hamad, E. K., Nady, G. (2019). Bandwidth Extension of Ultra-wideband Microstrip Antenna Using Metamaterial Double-side Planar Periodic Geometry. *Radio Engineering*, *28*(1), 25-32.

Haque, A., Reza, A. W., Kumar, N. (2015). A novel design of circular edge bow-tie nano antenna for energy harvesting. *Frequenz*, *69*(11-12), 491-499.

Karimzadeh Baee, R., Dadashzadeh, G., Kharakhili, F. G. (2007, December). Using of CSRR and its equivalent circuit model in size reduction of microstrip antenna. In *2007 Asia-Pacific Microwave Conference* (pp. 1-4). IEEE.

Kawdungta, S., Jaibanauem,P., Pongga, R., Phongcharoenpanich, C. (2017). Superstrate-integrated switchable beam rectangular microstrip antenna for gain enhancement. Radioengineering, 26(2), 430-437.

Khoomwong, E., Phongcharoenpanich, C. (2017). Simple and low-cost dual-band printed microwave absorber for 2.4-and 5-Ghz-band applications. *Frequenz*, *71*(11-12), 591-600.

Li, Z., Su, J., Li, Z. (2016, October). Design of high-gain lens antenna based on phase-gradient metasurface. In *2016 11th International Symposium on Antennas, Propagation and EM Theory (ISAPE)* (pp. 135-138). IEEE.

Mamilla, V. R., Chakradhar, K. S. (2014). Micro machining for micro electro mechanical systems (MEMS). *Procedia materials science*, *6*, 1170-1177.

Mark, R., Das, S. (2020). Near Zero Parameter Metamaterial Inspired Superstrate for Isolation Improvement in MIMO Wireless Application. *Frequenz*, *74*(1-2), 17-23.

Mishra, N. K., Das, S., Vishwakarma, D. K. (2019). Wideband High Gain Cylindrical Dielectric Resonator Antenna for X-Band Applications. *Frequenz*, *73*(3-4), 109-116.Pendry, J. B., Holden, A. J., Robbins, D. J., Stewart, W. J. (1999). Magnetism from conductors and enhanced nonlinear phenomena. *IEEE Transactions on Microwave Theory and Techniques*, *47*(11), 2075-2084.

Orazbayev, B., Beruete, M., Pacheco-Pena, V., Crespo, G., Teniente, J., Navarro-Cia, M. (2015). Soret fishnet metalens antenna. *Scientific reports*, *5*(1), 1-7.

Pen, T., Huang, B., Sun, H., Sun, X., Li, L. (2019). Broad-Band Substrate-Free Planar Metamaterial Lens Based on a Geometric Transformation of Polygon. *Frequenz*, *73*(9-10), 331-337.

Reddy, A. N., Raghavan, S. (2013, March). Split ring resonator and its evolved structures over the past decade: This paper discusses the nuances of the most celebrated composite particle (split-ring resonator) with which novel artificial structured materials (called metamaterials) are built. In *2013 IEEE International Conference ON Emerging Trends in Computing, Communication and Nanotechnology (ICECCN)* (pp. 625-629). IEEE.

Sabah, C., Roskos, H. G. (2012). Terahertz sensing application by using planar split-ring-resonator structures. Microsystem technologies, 18(12), 2071-2076.

Salamin, M. A., Das, S., Zugari, A. (2020). Closed Loop Resonator Based Compact UWB Antenna with Single Notched Band Varying between WLAN and X-band for UWB Applications. *Frequenz*, *1*(ahead-of-print).

Sauleau, R., Fernandes, C. A., Costa, J. R. (2005, June). Review of lens antenna design and technologies for mm-wave shaped-beam applications. In *11th International Symposium on Antenna Technology and Applied Electromagnetics [ANTEM 2005]* (pp. 1-5). IEEE.

Schurig, D., Mock, J. J., Justice, B. J., Cummer, S. A., Pendry, J. B., Starr, A. F., Smith, D. R. (2006). Metamaterial electromagnetic cloak at microwave frequencies. *Science*, *314*(5801), 977-980.

Smith, D. R., Kroll, N. (2000). Negative refractive index in left-handed materials. *Physical review letters*, *85*(14), 2933.

Smith, D. R., Pendry, J. B., Wiltshire, M. C. (2004). Metamaterials and negative refractive index. *Science*, *305*(5685), 788-792.

Talai, A., Gold, G., Frank, M., Mann, S., Weigel, R., Koelpin, A. (2017). A coplanar waveguide resonator based in-line material characterization sensor for bulk and metallized dielectrics. *Frequenz*, *71*(3-4), 173-183.

Wang, H., Sivan, V. P., Mitchell, A., Rosengarten, G., Phelan, P., Wang, L. (2015). Highly efficient selective metamaterial absorber for high-temperature solar thermal energy harvesting. *Solar Energy Materials and Solar Cells*, *137*, 235-242.

Veselago, V. G. (1968). The Electrodynamics of Substances with Simultaneously Negative Values of $\boldsymbol{\varepsilon}$ and $\boldsymbol{\mu}$.*Physics-Uspekhi*, *10*(4), 509-514.

Zeng, Y. C., Zhang, H., Min, X. L., Zhang, Y. (2019). A Triple Band-Notched UWB Antenna Using Folded Resonators. *Frequenz*, *73*(1-2), 37-43.